Available online at www.sciencedirect.com
ScienceDirect
Trans. Nonferrous Met. Soc. China 28(2018) 515−523
Transactions of Nonferrous Metals Society of China
www.tnmsc.cn

Superelastic properties of nanocrystalline NiTi shape memory alloy produced by thermomechanical processing

E. MOHAMMAD SHARIFI[1], A. KERMANPUR[2]

1. Department of Materials Engineering, Malek Ashtar University of Technology, Shahin Shahr, Isfahan, Iran;
2. Department of Materials Engineering, Isfahan University of Technology, Isfahan, Iran

Received 28 January 2017; accepted 10 May 2017

Abstract: Effects of thermomechanical treatment of cold rolling followed by annealing on microstructure and superelastic behavior of the $Ni_{50}Ti_{50}$ shape memory alloy were studied. Several specimens were produced by copper boat vacuum induction melting. The homogenized specimens were hot rolled and annealed at 900 °C. Thereafter, annealed specimens were subjected to cold rolling with different thickness reductions up to 70%. Transmission electron microscopy revealed that the severe cold rolling led to the formation of a mixed microstructure consisting of nanocrystalline and amorphous phases in $Ni_{50}Ti_{50}$ alloy. After annealing at 400 °C for 1 h, the amorphous phase formed in the cold-rolled specimens was crystallized and a nanocrystalline structure formed. Results showed that with increasing thickness reduction during cold rolling, the recoverable strain of $Ni_{50}Ti_{50}$ alloy was increased during superelastic experiments such that the 70% cold rolled−annealed specimen exhibited about 12% of recoverable strain. Moreover, with increasing thickness reduction, the critical stress for stress-induced martensitic transformation was increased. It is noteworthy that in the 70% cold rolled−annealed specimen, the damping capacity was measured to be 28 J/cm^3 that is significantly higher than that of commercial NiTi alloys.

Key words: nanocrystalline material; shape memory alloy; superelasticity; thermomechanical processing

1 Introduction

NiTi shape memory alloy (SMA) is one of the most important engineering materials which possesses two unique properties named superelasticity and shape memory effect [1,2]. Shape memory effect of NiTi SMA refers to its ability to recover original shape when it is heated to the temperature above the austenite finish temperature (A_f) after experiencing a certain deformation in the martensitic phase. Superelasticity of NiTi SMA refers to its nonlinear recoverable deformation behavior at the temperature above A_f, which is attributed to the stress-induced martensite transformation under loading and the spontaneous reversion of the transformation under unloading [3,4]. In addition to mentioned characteristics, NiTi SMA has high corrosion resistance, favorable biocompatibility and high damping capacity. Therefore, it has been employed in many applications including biomedical, aerospace, oil–gas, automotive, robotics and telecommunication industries [5]. The functional properties of SMA such as the recovery strain, shape recovery rate, recovery stress, temperature range of shape recovery and transformation yield stress, are structure-sensitive ones. Therefore, various thermomechanical treatments like cold rolling and subsequent annealing causing a well-developed dislocation substructure or nanocrystalline structure are effectively used for improving the superelastic properties of SMAs [6−8]. Cold rolling improves the superelastic behavior with increasing the critical stress for dislocations slip relative to critical stress for twinning mechanism [1]. Besides, NiTi shape memory alloys are prone to be amorphous by cold rolling. Post deformation annealing will result in the formation of a nanocrystalline structure if the optimum thermomechanical course is selected [6−8]. Nanocrystalline shape memory alloys have superior properties over their coarse grained counterparts. PROKOFIEV et al [9] reported that the formation of nanocrystalline structure in NiTi led to a higher strength of the alloy, with the effect on superelasticity, narrow hysteresis and low residual strain. RYKLINA et al [10] have shown that the nanostructures in NiTi alloy led to increasing the recovery strain as

Corresponding author: E. MOHAMMAD SHARIFI; Tel: +98-3145912501; Fax: +98-3145228530; E-mail: ehsan_sharifi_2000@yahoo.com
DOI: 10.1016/S1003-6326(18)64684-9

compared to the coarse-grained counterparts. MEI et al [11] demonstrated that the elastic modulus of nanostructured NiTi increases dramatically. TSUCHIYA et al [12] produced nanocrystalline NiTi wire with high tensile strength and high elastic modulus. DELVILLE et al [13] and MALARD et al [14] prepared nanostructured NiTi wire by means of cold drawing and heat treatments. They found that the NiTi wire with nanocrystalline structure possesses perfect superelasticity with a recoverable strain of 8%.

The tensile properties and transformation behavior of the nanostructured $Ti_{50}Ni_{50}$ shape memory alloy prepared by copper boat induction melting followed by thermomechanical treatment were discussed in previous works [15,16]. In the current research, the effect of thermomechanical processing comprised cold rolling followed by annealing on the superelastic properties of an equiatomic NiTi shape memory alloy is investigated.

2 Experimental

$Ni_{50}Ti_{50}$ (mole fraction, %) cast ingots were prepared by a home-made copper-boat vacuum induction melting system. The as-cast cylindrical ingots were homogenized at 900 °C for 4 h in a vacuum furnace followed by cold water quenching. After homogenization, the ingots were hot rolled at 900 °C into a sheet of 2.5 mm in thickness and then annealed at 900 °C for 1 h followed by water quenching. The annealed specimens were cold rolled with 20%−70% thickness reduction at room temperature. Based on the crystallization temperatures determined from calorimetric measurements, post deformation annealing was conducted at 400 °C for 1 h in vacuum.

Transformation behavior and microstructure evolution of the $Ni_{50}Ti_{50}$ alloy were investigated by means of differential scanning calorimetry (DSC NETZSCH 200F3), X-ray diffraction (XRD Philips X'Pert with Cu K_α radiation) and field emission transmission electron microscopy (TEM JEOL−2100F) techniques. DSC measurements were made with a cooling and heating rate of 10 °C/min. The crystallite size, residual microstrain and dislocation density of all samples which were subjected to various cold reductions are determined by analyzing the XRD patterns via the Rietveld software, Materials analysis using diffraction (MAUD) [17]. Details of method of analysis have been reported elsewhere [17−20]. After fitting the theoretical curve on the XRD pattern of samples, related values of microstructural parameters (such as crystallite size and microstrain) for each XRD peak were provided by software. The value of the dislocation density (ρ) was calculated [21] from the average values of the crystallite size (D) and microstrain $(\varepsilon^2)^{0.5}$ (output data of MAUD software) by the following equation:

$$\rho = \frac{3\sqrt{2\pi}(\varepsilon^2)^{0.5}}{Db} \tag{1}$$

where b is the absolute value of Burgers vector.

Samples for TEM were prepared by polishing with a twin-jet electro-polisher (Struers, Tenupol-5) in a solution of 90% acetic acid glacial and 10% perchloric acid at 15 °C under 35 V. TEM observations were made at the operating voltage of 200 kV. Tensile test was carried out according to ASTM-F2516 (standard test method for tension testing of nickel−titanium superelastic materials) with a strain rate of 1×10^{-3} s^{-1} at room temperature. All tensile test specimens were cut along the rolling direction.

3 Results and discussion

The as-homogenized microstructure was composed of coarse grains with an average size of 50 μm. The XRD results show that the homogenized NiTi specimen consists of $B2$ austenite and $B19'$ martensite phases. DSC curves of the homogenized specimen are shown in Fig. 1. In this figure, DSC peaks corresponding to the $B2$−$B19'$ on cooling and the reverse $B19'$−$B2$ transformation on heating are clearly seen (M_s=54 °C, M_f=26 °C, A_s=61 °C, A_f=93 °C). It should be noted that the two-phase microstructure of the homogenized sample, as characterized by XRD at room temperature, is not consistent with the transformation temperatures, determined by DSC. The reason is believed to be due to the higher cooling rate (about 10000 °C/min) during quenching from the homogenization temperature compared with the one used in the DSC test (e.g. 10 °C/min) [15,16]. As already reported by CHANG et al [22], the M_f is significantly reduced by increasing the cooling rate. As a consequence, a complete $B2$ to $B19'$ transformation may not take place during the quenching stage leading to the two phase microstructure.

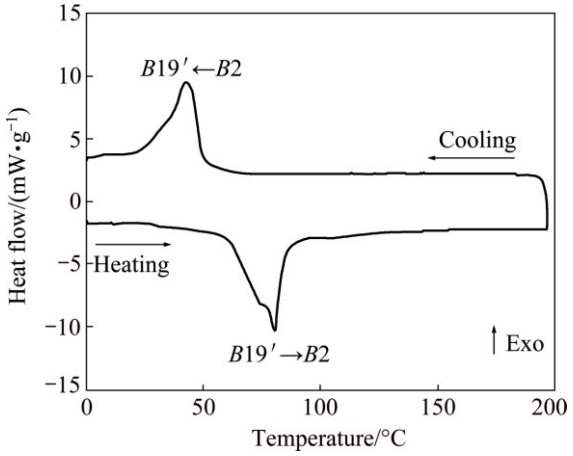

Fig. 1 DSC curves of homogenized $Ni_{50}Ti_{50}$ specimen

Cold rolling of $Ni_{50}Ti_{50}$ alloy led to significant peak broadening in X-ray diffraction pattern as a result of crystal refinement and introduction of high density of dislocations [23]. Peak broadening would also be related to the occurrence of amorphization as a result of subjecting the alloy to severe plastic deformation [24]. The average crystallite size and microstrain of cold rolled specimens with various thickness reductions which calculated by MAUD software are given in Table 1. It is noticed that the cold rolling reduces the crystallite size and increases the microstrain. In Fig. 2 the calculated values of dislocation density (from the data of Table 1 and Eq. (1)) are presented. It can be seen that dislocation density is increased to 1.03×10^{13} cm^{-2} with increasing thickness reduction up to 70%. Similar results were reported by KOIKE et al [25]. They estimated an extremely high dislocation density of 10^{13} to 10^{14} cm^{-2} in cold rolled NiTi, and suggested that this dislocation density is a major driving force for amorphization in cold rolled NiTi.

Table 1 Average values of crystallite size (D) and microstrain (ε) of cold rolled specimens with various thickness reductions

Thickness reduction/%	D/Å	ε
20	54	0.00364
30	44	0.00514
40	42	0.00693
50	39	0.00707
60	35	0.00895
70	25	0.01029

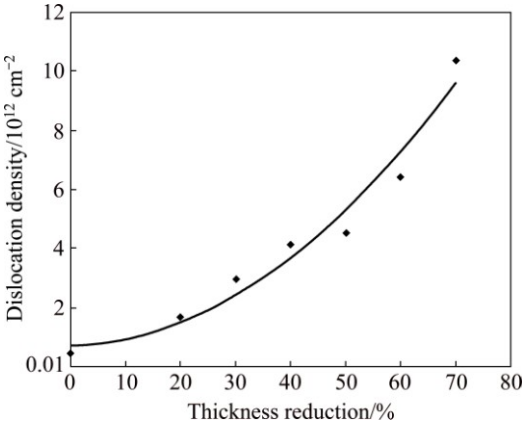

Fig. 2 Calculated dislocation density as function of thickness reduction in cold rolled $Ni_{50}Ti_{50}$ specimen

Figure 3 shows the TEM bright-field image and corresponding selected area diffraction pattern (SADP) of the cold rolled $Ni_{50}Ti_{50}$ specimen by 40% reduction. Figure 3(a) illustrates the high density arrays of dislocations which seem to define original twin boundaries in the stress-induced martensite during cold rolling. However, the SADP shown in Fig. 3(b) indicates that the structure is mainly nanocrystalline $B2$ austenite and amorphous phase. Therefore, it can be inferred that the initial deformation mechanism of this alloy during cold rolling is stress-induced martensitic transformation followed by plastic deformation of martensite via dislocation slip and subsequent martensite to austenite transformation via the reverse transformation after cold rolling (unloading) [15,16]. Twin boundary movement and dislocation slip are the most important deformation modes in martensitic phase of NiTi [26]. These twin boundaries will act as the barriers for the motion of dislocations during deformation and promote their high density accumulation. Figure 4 shows a schematic

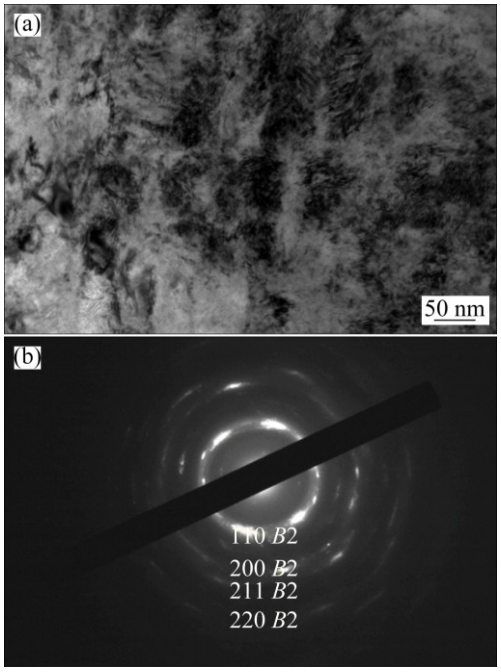

Fig. 3 Bright-field TEM image (a) and corresponding diffraction pattern (b) of 40% cold rolled $Ni_{50}Ti_{50}$ specimen

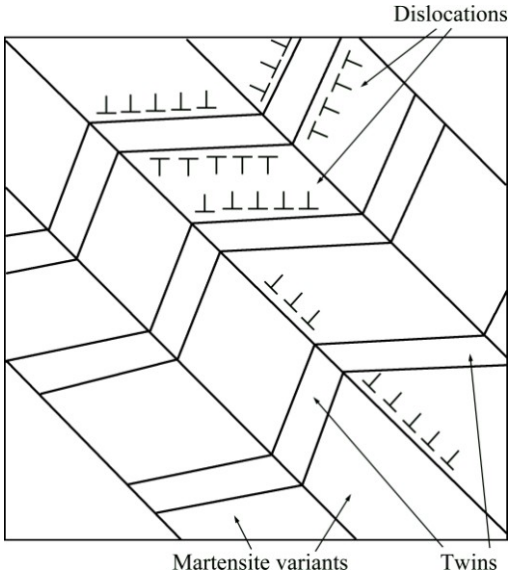

Fig. 4 Schematic illustration of accumulation of dislocations along twin and variant boundaries in martensite during plastic deformation of NiTi alloy

illustration of the accumulation of dislocations along twin and variant boundaries in martensite during plastic deformation of NiTi alloy [27].

TEM bright-field image and corresponding SADPs of the microstructure of the 70% cold rolled specimen are shown in Fig. 5. In Fig. 5(a), the bands with no marked contrast running from lower right to upper left corner are inferred to be an amorphous region and other areas surrounding the amorphous band illustrate complex strain contrast and appear to be a nanocrystalline phase. Figures 5(b) and (c) are the SADPs obtained from the amorphous and nanocrystalline regions denoted by letters *A* and *N* on the bright field image, respectively. Only a diffuse ring corresponding to an amorphous phase is found in the SADP of Fig. 5(b), while discrete diffraction rings of the *B*2 parent phase and a diffuse ring are found simultaneously in Fig. 5(c). As a result, it can be say that the region *A* is purely amorphous, while the region *N* is a mixture of amorphous and nanocrystalline *B*2 phases. Thus, it can be mentioned that along with the occurrence of high density accumulation of dislocations

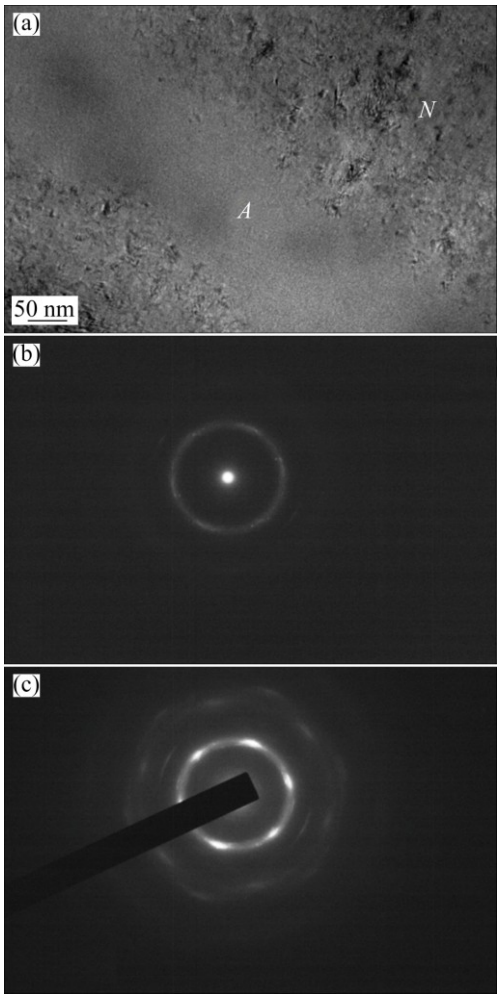

Fig. 5 TEM images of 70% cold rolled $Ni_{50}Ti_{50}$ specimen: (a) Bright field image; (b, c) Diffraction patterns corresponding to *A* and *N* in (a), respectively

and the interaction between them, the cold rolled specimen is gradually subjected to nanocrystallization. By increasing the cold deformation, the dislocation density becomes greater than a critical value, beyond which the nanocrystalline phase is further subjected to amorphization [15,16,25]. Similar band shaped amorphous phase was observed in high pressure torsion processed NiTi alloy [28]. PETERLECHNER et al [28] observed that ultrathin amorphous ribbons formed at grain boundaries are intersected by shear bands. At higher deformation, these ribbons are transformed into thicker amorphous bands containing nanocrystalline debris. JIANG et al [3] studied the effect of severe plastic deformation via local canning compression on the microstructural evolutions of binary $Ni_{50.9}Ti_{49.1}$ alloy and they reported similar experimental findings. They concluded that deformation mechanism of NiTi alloy under local canning compression involves stress-induced martensite transformation, deformation twinning, dislocation slip, nanocrystallization and amorphization. They have shown that the critical dislocation density plays a predominant role in the occurrence of the amorphous phase in the deformed $Ni_{50.8}Ti_{49.2}$ sample. KARAMAN et al [27] studied the effect of severe plastic deformation via equal channel angular extrusion (ECAE) on the deformation behavior of NiTi alloy. They reported that a high volume fraction of twin-related nanograins was formed in *B*2 phase after ECAE processing. It was thought to be a consequence of a set of mechanisms including stress-induced martensitic transformation, deformation twinning in martensite and reverse transformation to *B*2 phase [27].

DSC curves of the 40% and 70% cold rolled specimens are shown in Fig. 6. No transformation peak can be seen in these curves in the temperature range which is shown in DSC profile (compared with Fig. 1). This is the result of the introduction of dislocations, elastic strain and crystal refinement during rolling that depresses martensitic transformation temperatures and stabilizes austenite phase [23]. Because the martensitic transformation involves a large amount of shear, any strengthening mechanism that can hinder the transformation shear, can lower transformation temperatures. This feature can be expressed by [29]

$$M_s=T_0-K\sigma_y \quad (2)$$

where the constant K is the factor of proportionality between the critical shear stress and the yield stress σ_y, as well as all the transformable properties. In Eq. (2), the equilibrium temperature T_0 is a function of the chemical composition, and the yield stress σ_y is proportional to the strength of austenite phase. In the present work, the cold rolling process does not change the composition; hence, T_0 is a constant. In addition, cold rolling can strengthen

the NiTi alloy by causing retained dislocations, and therefore, can raise the yield stress σ_y. As derived from Eq. (1), this feature should cause M_s and corresponding transformation temperatures to be lowered by cold rolling [29].

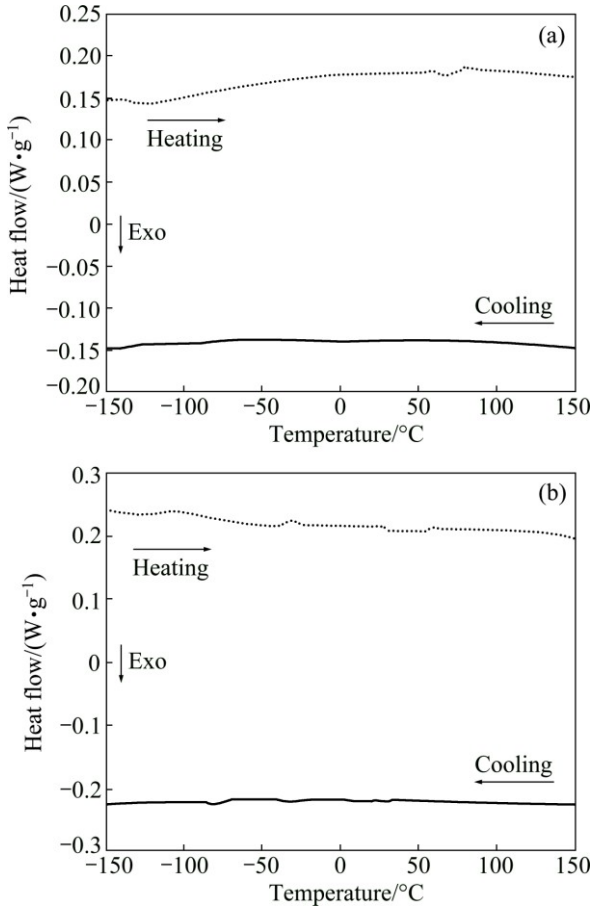

Fig. 6 DSC curves of 40% (a) and 70% (b) cold rolled $Ni_{50}Ti_{50}$ specimens

Based on the crystallization temperatures determined from the DSC measurements of the cold rolled specimens during heating up to the temperature of 500 °C (not shown), annealing treatment was performed at 400 °C for 1 h in vacuum in order to crystallize the amorphous phase. TEM bright-field images of the 40% cold rolled $Ni_{50}Ti_{50}$ specimen after annealing at 400 °C are shown in Fig. 7. Moreover, in Fig. 8, TEM bright-field image and SADP are presented for $Ni_{50}Ti_{50}$ alloy subjected to 70% cold-rolling followed by annealing at 400 °C for 1 h. The grain size of the 40% cold rolled and annealed specimen is 30−140 nm, whereas it is 20−70 nm for the 70% cold rolled and annealed one. This shows the correlation between the final grain size and the thickness reduction during cold rolling prior to annealing treatment. As shown in Fig. 8(b), the SADP of the 70% cold rolled and annealed specimen is identified as the austenite and martensite phases with no diffuse rings corresponding to the amorphous phase, showing the completion of crystallization. These are in agreement with the XRD results [15,16].

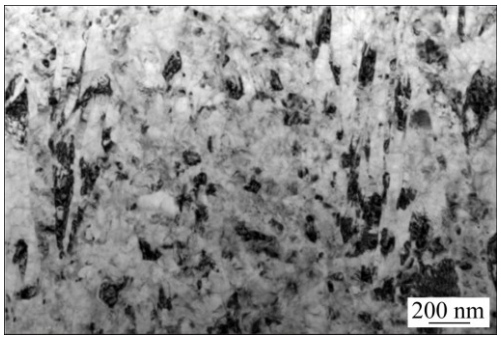

Fig. 7 Bright-field TEM image of 40% cold rolled $Ni_{50}Ti_{50}$ specimen after annealing at 400 °C for 1 h

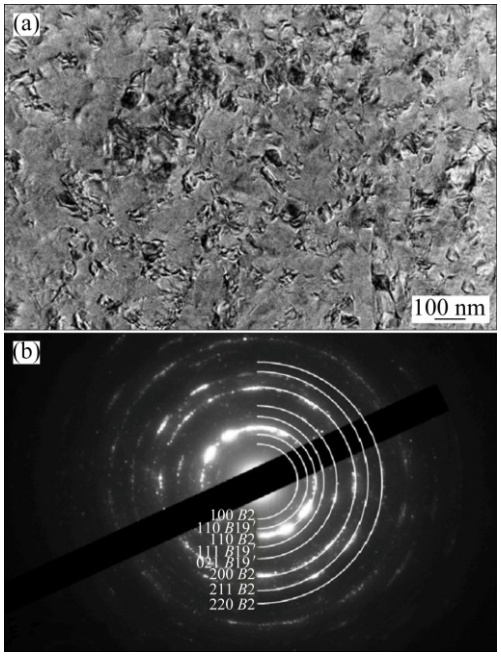

Fig. 8 Bright-field TEM image (a) and corresponding diffraction pattern (b) of 70% cold rolled $Ni_{50}Ti_{50}$ specimen after annealing at 400 °C for 1 h

Figure 9 shows the thermal transformation behavior of the 40% and 70% cold rolled $Ni_{50}Ti_{50}$ specimens annealed at 400 °C. Unlike the cold rolled specimens whose DSC curves exhibited no transformation peak, annealed specimens showed a one-stage $B2 \rightarrow B19'$ transformation on cooling and a two-stage $B19' \rightarrow R \rightarrow B2$ transformation on heating. This implies that the post deformation annealing annihilates dislocations generated during deformation which locked the austenite−martensite transformation interfaces and as a result the martensitic transformation emerges again in subsequent thermal cycles [15,16,23].

Tensile stress–strain curves of the $Ni_{50}Ti_{50}$ specimens cold rolled up to 70% followed by post deformation annealing at 400 °C are presented in Fig. 10.

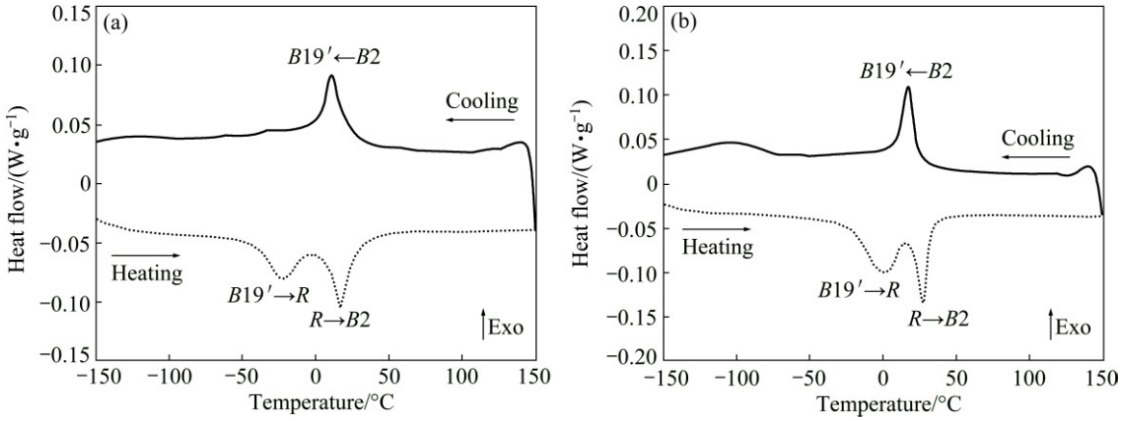

Fig. 9 DSC curves of 40% (a) and 70% (b) cold rolled $Ni_{50}Ti_{50}$ specimens after annealing at 400 °C for 1 h

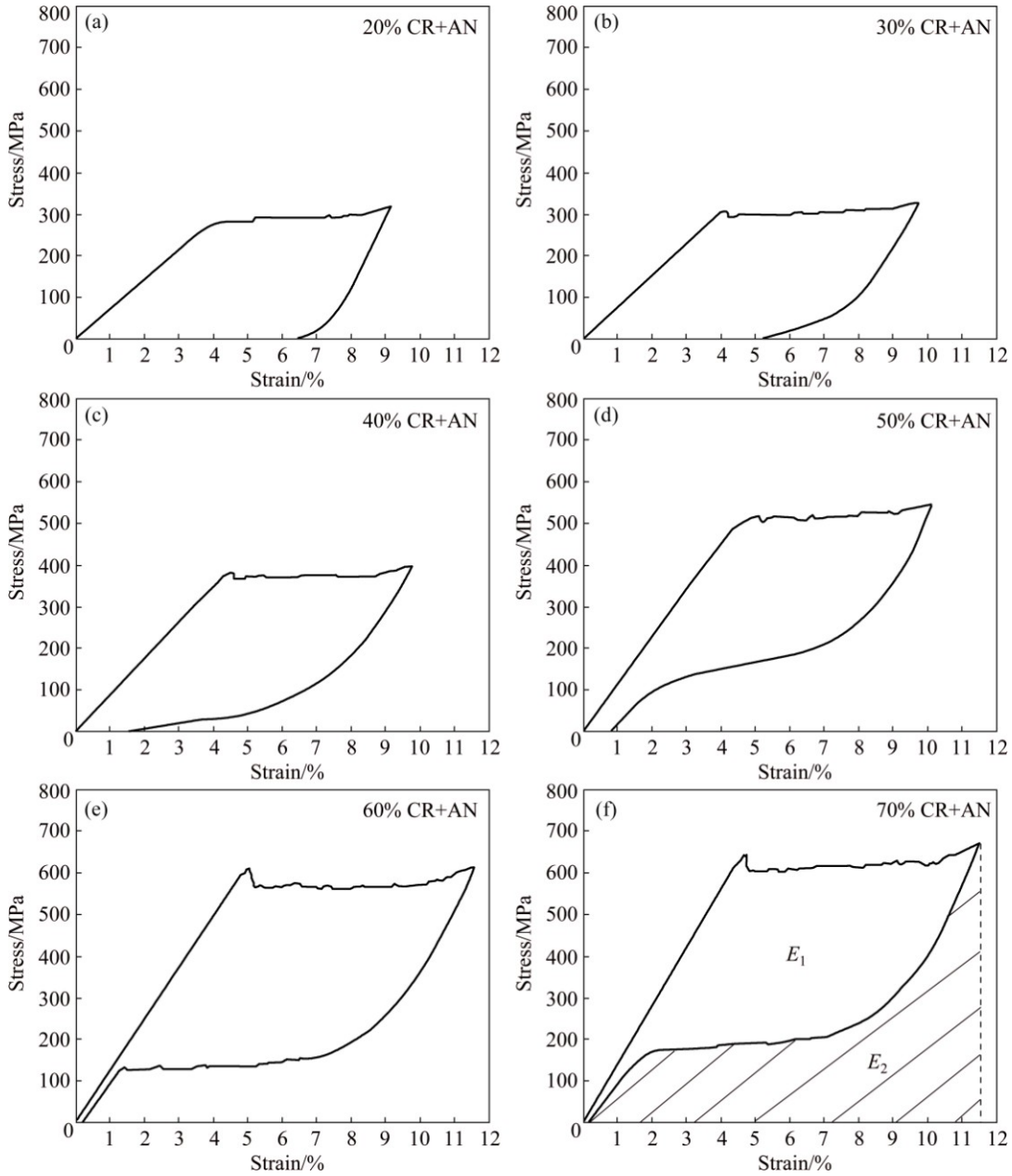

Fig. 10 Engineering tensile stress−strain curves of cold rolled $Ni_{50}Ti_{50}$ specimens with various thickness reductions after annealing at 400 °C for 1 h (CR—Cold rolling; AN—Annealing)

The main feature of the stress−strain curves of the annealed specimens is the appearance of the plateau region corresponding to the stress-induced martensitic transformation which is a basic characteristic of functional superelastic alloys. During annealing, rearrangement of random dislocations which were introduced during rolling and crystallization of amorphous phase takes place. As a result, dislocation free nanograins are formed in the microstructure after post deformation annealing (see Fig. 7 and Fig. 8). The nanocrystalline structure provides the necessary strength to the austenite phase to avoid plastic deformation by slip mechanism and as a result stress-induced martensitic transformation could occur during tensile loading [15,16,30]. Figure 11 shows changes in the upper plateau stress, which shows critical stress for stress-induced martensitic transformation (σ_{SIM}), and the residual (irrecoverable) strain with increasing thickness reduction in cold rolling. It is observed that the stress level of the upper plateau is significantly improved by increasing thickness reduction during cold rolling. It is noteworthy that in the 70% cold rolled-annealed specimen, the value of σ_{SIM} was measured as high as 610 MPa which is significantly higher than that of the coarse-grained $Ni_{50}Ti_{50}$ alloy (160 MPa) [31]. Moreover, with increasing thickness reduction, the irrecoverable strain (ε_R) of nanostructured $Ni_{50}Ti_{50}$ alloy was decreased during superelastic experiments such that the 70% cold rolled-annealed specimen exhibited about 12% of recoverable strain which is significantly higher than that of the coarse-grained $Ni_{50}Ti_{50}$ shape memory alloy (~8%) [1]. The observed improvement in the superelastic behavior of the $Ni_{50}Ti_{50}$ alloy can be attributed to the enhancement of the critical dislocation-induced slip stress as a result of grain size reduction and formation of nanocrystalline structure [32]. As seen in Figs. 7 and 8, the annealed specimen with the higher thickness reduction (70%) had smaller grain size compared with the annealed specimen with lower thickness reduction (40%). The microstructure with smaller grain size provides a higher density of grain boundaries and the necessary strength to the austenite phase to avoid plastic deformation by slip mechanism and as a result stress-induced martensitic transformation could occur during tensile loading [30].

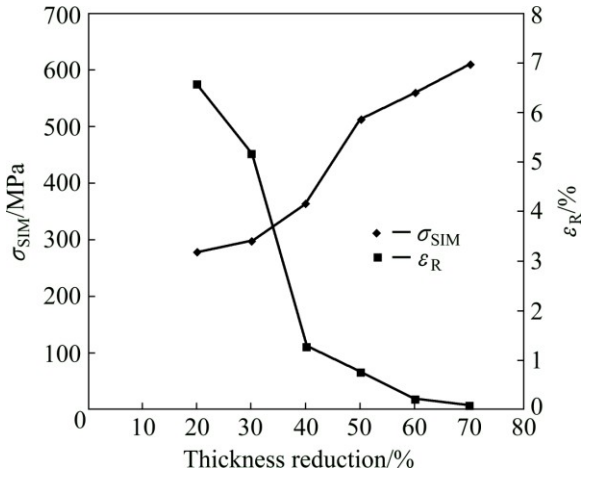

Fig. 11 Variations of upper plateau stress (σ_{SIM}) and residual strain (ε_R) versus thickness reduction for cold-rolled and annealed $Ni_{50}Ti_{50}$ specimens

The origin of mechanical hysteresis in superelastic curves is related to the friction energy which originates from the austenite/martensite interface motion [5]. In Fig. 10, the area E_1 represents the energy density per unit volume which is dissipated during one complete cycle, while E_2 is the energy density per unit volume which is stored and available to release upon unloading. The nanostructured $Ni_{50}Ti_{50}$ alloy has considerable damping capacity (E_D), which in simple terms is the ability to repeatedly disperse unwanted energy from a system. Damping capacity is related to the mechanical hysteresis and transformation strain and can be determined by calculating the area between the forward and reverse transformations in the superelastic stress–strain curves (E_D=E_1). High hysteresis and transformation strain result in more energy dissipation from a system [33]. It is noteworthy that in the 70% cold rolled-annealed specimens, E_D was measured to be 28 J/cm^3 which is significantly higher than that of commercial NiTi alloys (10 J/cm^3) [33]. So, because of their energy-absorbing capabilities, nanocrystalline $Ni_{50}Ti_{50}$ SMA, could be employed as dampers in aerospace (in aircraft engines to dampen acoustic energy) and construction (in impact damping devices to counter seismic movements) industries.

4 Conclusions

1) After the post-deformation annealing of the 70% cold rolled specimen at 400 °C for 1 h, an entirely nanocrystalline structure with the grain size within 20−70 nm was achieved in $Ni_{50}Ti_{50}$ alloy.

2) Superelastic behavior of $Ni_{50}Ti_{50}$ alloy could be significantly improved through grain refinement and formation of nanocrystalline structure.

3) With increasing thickness reduction during cold rolling, the recoverable strain of $Ni_{50}Ti_{50}$ alloy was increased during superelastic experiments such that the 70% cold rolled−annealed specimen exhibited about 12% of recoverable strain. In addition, with increasing thickness reduction, the critical stress for stress-induced martensitic transformation was increased.

4) The nanocrystalline $Ni_{50}Ti_{50}$ alloy had a high damping capacity of 28 J/cm^3.

References

[1] OTSUKA K, WAYMAN C M. Shape memory materials [M]. Cambridge: Cambridge University Press, 1998.

[2] KHALEGHI F, KHALIL-ALLAFI J, ABBASI-CHIANEH V, NOORI S. Effect of short-time annealing treatment on the superelastic behavior of cold drawn Ni-rich NiTi shape memory wires [J]. J Alloys Compd, 2013, 554: 32−38.

[3] JIANG S Y, TANG M, ZHAO Y, HU L, ZHANG Y, LIANG Y. Crystallization of amorphous NiTi shape memory alloy fabricated by severe plastic deformation [J]. Transactions of Nonferrous Metals Society of China, 2014, 24: 1758−1765.

[4] OTSUKA K, REN X. Physical metallurgy of Ti–Ni-based shape memory alloys [J]. Prog Mater Sci, 2005, 50: 511−678.

[5] JANI J M, LEARY M, SUBIC A, GIBSON M A. A review of shape memory alloy research, applications and opportunities [J]. Mater Des, 2014, 56: 1078−1113.

[6] BRAILOVSKI V, PROKOSHKIN S, INAEKYAN K, DEMERS V. Functional properties of nanocrystalline, submicrocrystalline and polygonized Ti−Ni alloys processed by cold rolling and post-deformation annealing [J]. J Alloys Compd, 2011: 509: 2066−2075.

[7] FACCHINELLO Y, BRAILOVSKI V, PROKOSHKIN S D, GEORGES T, DUBINSKIY S M. Manufacturing of nanostructured Ti−Ni shape memory alloys by means of cold/warm rolling and annealing thermal treatment [J]. J Mater Process Technol, 2012, 212: 2294−2304.

[8] PROKOSHKIN S D, BRAILOVSKI V, INAEKYAN K E, DEMERS V, KHMELEVSKAYA I Y, DOBATKIN S V, TATYANIN E V. Structure and properties of severely cold-rolled and annealed Ti−Ni shape memory alloys [J]. Mater Sci Eng A, 2008, 481−482: 114–118.

[9] PROKOFIEV E, BUROW J, FRENZEL J, GUNDEROV D, EGGELER G, VALIEV R. Phase transformations and functional properties of NiTi alloy with ultrafine-grained structure [J]. Mater Sci Forum, 2011, 667−669: 1059−1064.

[10] RYKLINA E P, PROKOSHKIN S D, KREYTSBERG A Y. Abnormally high recovery strain in Ti−Ni-based shape memory alloys [J]. J Alloys Compd, 2013, 577: 255−258.

[11] MEI Q S, ZHANG L, TSUCHIYA K, GAO H, OHMURA T, TSUZAKI K. Grain size dependence of the elastic modulus in nanostructured NiTi [J]. Scr Mater, 2010, 63: 977−980.

[12] TSUCHIYA K, HADA Y, KOYANO T, NAKAJIMA K, OHNUMA M, KOIKE T, TODAKA Y, UMEMOTO M. Production of TiNi amorphous/nanocrystalline wires with high strength and elastic modulus by severe cold drawing [J]. Scripta Mater, 2009, 60: 749−752.

[13] DELVILLE R, MARALD B, PILCH J, SITTNER P, SCHRYVERS D. Microstructure changes during non-conventional heat treatment of thin Ni−Ti wires by pulsed electric current studied by transmission electron microscopy [J]. Acta Mater, 2010, 58: 4503−4515.

[14] MARALD B, PILCH J, SITTNER P, DELVILLE R, CURFS C. In situ investigation of the fast microstructure evolution during electropulse treatment of cold drawn NiTi wires [J]. Acta Mater, 2011, 59: 1542−1556.

[15] MOHAMMAD SHARIFI E, KERMANPUR A, KARIMZADEH F, ESMAILI A. Formation of the nanocrystalline structure in an equiatomic NiTi shape-memory alloy by thermomechanical processing [J]. J Mater Eng Perform, 2014, 23: 1408−1421.

[16] MOHAMMAD SHARIFI E, KARIMZADEH F, KERMANPUR A. The effect of cold rolling and annealing on microstructure and tensile properties of the nanostructured $Ni_{50}Ti_{50}$ shape memory alloy [J]. Mater Sci Eng A, 2014, 607: 33−37.

[17] LUTTEROTTI L. MAUD: Material analysis using diffraction [EB/OL]. http://www.ing.unitn.it/~maud/.

[18] CHANDA A, DE M. X-ray characterization of the microstructure of α-CuTi alloys by Rietveld's method [J]. J. Alloys Compd, 2000, 313: 104−114.

[19] MURUGESAN S, KUPPUSAMI P, MOHANDAS E, VIJAYALAKSHMI M. X-ray diffraction Rietveld analysis of cold worked austenitic stainless steel [J]. Mater Lett, 2012, 67: 173−176.

[20] SAHU P, DE M, KAJIWARA S. Microstructural characterization of stress-induced martensites evolved at low temperature in deformed powders of Fe−Mn−C alloys by the Rietveld method [J]. J Alloys Compd, 2002, 346: 158−169.

[21] DINI G, UEJI R, NAJAFIZADEH A, MONIR-VAGHEFI S M. Flow stress analysis of TWIP steel via the XRD measurement of dislocation density [J]. Mater Sci Eng A, 2010, 527: 2759−2763.

[22] CHANG S H, WU S K, Effect of cooling rate on transformation temperature measurements of $Ti_{50}Ni_{50}$ alloy by differential scanning calorimetry and dynamic mechanical analysis [J]. Mater Charact, 2008, 59: 987−990.

[23] TSUCHIYA K, INUZUKA M, TOMUS D, HOSOKAWA A, NAKAYAMA H, MORII K, TODAKA Y, UMEMOTO M. Martensitic transformation in nanostructured TiNi shape memory alloy formed via severe plastic deformation [J]. Mater Sci Eng A, 2006, 438−440: 643−648.

[24] PROKOSHKIN S D, KHMELEVSKAYA I Y, DOBATKIN S V, TRUBITSYNA I B, TATYANIN E V, STOLYAROV V V, PROKOFIEV E A. Alloy composition, deformation temperature, pressure and post-deformation annealing effects in severely deformed Ti−Ni based shape memory alloys [J]. Acta Mater, 2005, 53: 2703−2714.

[25] KOIKE J, PARKIN D M, NASTASI M. Crystal-to-amorphous transformation of NiTi induced by cold rolling [J]. J Mater Res, 1990, 7: 1414−1418.

[26] JIANG S, HU L, ZHAO Y, ZHANG Y, LIANG Y. Multiscale investigation of inhomogeneous plastic deformation of NiTi shape memory alloy based on local canning compression [J]. Mater Sci Eng A, 2013, 569: 117−123.

[27] KARAMAN I, YAPICI G G, CHUMLYAKOV Y I, KIREEVA I V. Deformation twinning in difficult-to-work alloys during severe plastic deformation [J]. Mater Sci Eng A, 2005, 410−411: 243−247.

[28] PETERLECHNER M, WAITZ T, KARNTHALER H P Nanoscale amorphization of severely deformed NiTi shape memory alloys [J]. Scr Mater, 2009, 60: 1137−1140.

[29] LIN H C, WU S K. Effects of hot rolling on the martensitic transformation of an equiatomic Ti−Ni alloy [J]. Mater Sci Eng A, 1992, 158: 87−91.

[30] SAIKRISHNA C N, RAMAIAH K V, ALLAM PRABHU S, BHAUMIK S K. On stability of NiTi wire during thermo-mechanical cycling [J]. Bull Mater Sci, 2009, 32: 343−352.

[31] TSUCHIYA K, CAO Q, HOSOKAWA A, KATAHIRA M, TODAKA Y, UMEMOTO M. Nanostructured shape memory alloys for biomedical applications [J]. Mater Sci Forum, 2007, 539−543: 505−510.

[32] ZHANG H, LI X, ZHANG X. Grain-size-dependent martensitic transformation in bulk nanocrystalline TiNi under tensile deformation [J]. J Alloys Compd, 2012, 544: 19−23.

[33] KARACA H E, ACAR E, DED G S, BASARAN B, TOBE H, NOEBE R D, BIGELOW G, CHUMLYAKOV Y I. Shape memory behavior of high strength NiTiHfPd polycrystalline alloys [J]. Acta Mater, 2013, 61: 5036−5049.

形变热处理制备的纳米晶 NiTi 形状记忆合金的超弹性行为

E. MOHAMMAD SHARIFI[1], A. KERMANPUR[2]

1. Department of Materials Engineering, Malek Ashtar University of Technology, Shahin Shahr, Isfahan, Iran;
2. Department of Materials Engineering, Isfahan University of Technology, Isfahan, Iran

摘　要：研究冷轧和后续退火形变热处理对 $Ni_{50}Ti_{50}$ 形状记忆合金超弹性行为的影响。采用铜坩埚真空感应熔炼法制备样品。将成分均匀的样品进行热轧后在 900 °C 退火，然后再进行冷轧，冷轧后样品的厚度有不同程度的减少，最大可达 70%。透射电镜检测结果显示严重的冷轧导致 $Ni_{50}Ti_{50}$ 合金中形成了纳米晶和非晶的复合显微组织。400 °C 下退火 1 h 后，冷轧样品中的非晶发生晶化形成纳米晶组织。随着冷轧变形量的增加，在超弹性实验中 $Ni_{50}Ti_{50}$ 合金的弹性应变增加，变形量为 70%的冷轧−退火样品其弹性应变为 12%。此外，随着变形量的增加，应力诱导马氏体相变的临界应力提高。值得注意的是，70%变形量的冷轧−退火样品的阻尼容量值为 28 J/cm^3，明显高于商业 NiTi 合金。

关键词：纳米晶材料；形状记忆合金；超弹性；形变热处理

(Edited by Xiang-qun LI)